

Effective Field Theory in Nuclear Physics¹

Martin J. Savage

*Department of Physics, University of Washington,
Seattle, WA 98195*

and

*Jefferson Lab., 12000 Jefferson Avenue, Newport News,
Virginia 23606.*

Abstract. I review recent developments in the application of effective field theory to nuclear physics. Emphasis is placed on precision two-body calculations and efforts to formulate the nuclear shell model in terms of an effective field theory.

INTRODUCTION

A question that I have been asked many times is “*Why use Effective Field Theory in Nuclear Physics*”? The simple and somewhat glib answer to this question is that the only other option that one has to using an effective field theory (EFT) is to use the “*Theory of Everything*” (TOE), string theory or some derivative thereof. All other descriptions **must** be incomplete at some level and when precise predictions are compared with precise measurements, differences will become obvious. It is a daunting prospect for us (maybe only me) to use the TOE to compute low-energy hadronic processes, and in fact, it is quite silly to even consider such calculations. After all, we know that processes in QED can be computed to high precision which agree with experimental observations, without knowing anything about physics at the Planck scale, M_{pl} .

The renormalizability of QED assures that ultra-violet divergences, arising from our lack of understanding of physics at short-distances, can be explicitly removed by a few constants (electric charge and fermion mass), allowing observables to be related to each other to arbitrary precision. In contrast, EFT’s are non-renormalizable but are still predictive when a systematic power counting in small expansion parameters can be established. Relations between observables at a given

¹⁾ Talk presented at the *7th Conference on the Intersections of Particle and Nuclear Physics*, Quebec City, Canada, May 22-28, 2000. NT@UW-00-018.

precision will involve a finite number of constants that are not dictated by the symmetries of the EFT alone. For instance, the standard model is a renormalizable field theory but processes at energies much less than the scale of electroweak symmetry breaking can be described by a non-renormalizable EFT of reduced symmetry, $SU(3)_c \otimes SU(2)_L \otimes U_Y(1) \rightarrow SU(3)_c \otimes U_{\text{em}}(1)$, where weak interactions are incorporated by higher-dimension four-fermi operators. Even with quantum effects, the theory provides a systematic expansion of observables in terms of q^2/M_W^2 and m_f^2/M_W^2 , where m_f is a fermion mass, M_W is the mass of the weak gauge bosons, and q is the external momentum.

If one were interested in calculating the cross section for $np \rightarrow d\gamma$ —radiative neutron capture by a proton to form a deuteron—directly from QCD, then a lattice calculation is the only technique available. The lattice calculation will provide an unambiguous cross section in terms of the quark masses and Λ_{QCD} , or equivalently in terms of other hadronic observables. A cartoon of a contribution to $np \rightarrow d\gamma$ in terms of perturbative quarks and gluons is shown in Figure 1. Sources of quarks and

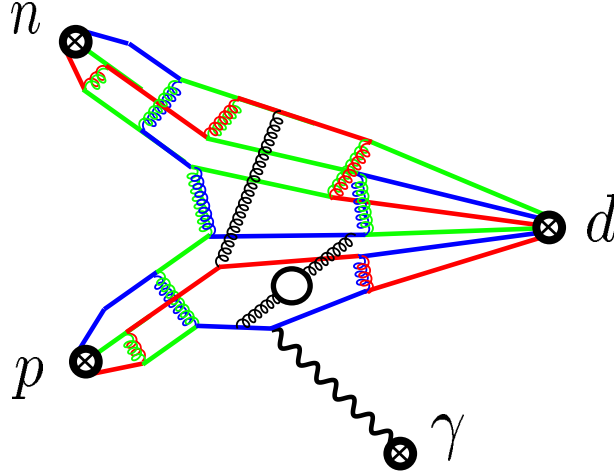


FIGURE 1. A “cartoon” of a contribution to $np \rightarrow d\gamma$ in QCD.

gluons that have non-zero overlap with the proton, neutron, deuteron and a source for the photon would be used to generate the amplitude for $np \rightarrow d\gamma$. It is clear that a significant amount of work goes into forming the hadronic states themselves, let alone computing the interaction terms. In addition, as the deuteron has such a small binding energy and hence is quite extended compared to the nucleon, considerable effort will be required to generate the deuteron itself. Unfortunately, at this point in time the lattice community is not even close to being able to perform this multi-hadron calculation. Indeed, the deuteron itself remains to be generated in lattice calculations.² If all nuclear length scales were of order the chiral symmetry break-

²⁾ During the *Effective Field Theory* workshop to be held at the *Institute for Nuclear Physics* at the *University of Washington* during the summer of 2000, efforts will be made to estimate the computer resources necessary to determine the deuteron binding energy from lattice QCD [1].

ing scale Λ_χ then (very) naively lattice computations of nuclear observables would not be that much harder than computations in the single-nucleon sector. However, there are several low-energy length scales that play important roles in nuclear physics. Firstly Λ_χ , below which a hadronic description makes sense, and higher-dimension operators are induced that describe contributions from scales above Λ_χ . Secondly, the scale of the repulsive part of the nucleon-nucleon interaction, which is conventionally modeled by the exchange of vector mesons (far from mass-shell) and numerically is of order Λ_χ . Thirdly, the mass of the pion, which is much less than Λ_χ due to its special status as a pseudo-Goldstone boson. Finally, nuclear binding energies which are much smaller than one would naively guess.

If one is interested in this process at energies much less than Λ_χ , or the mass of the ρ -meson, but comparable to the mass of the pion, then it should be sufficient to use an EFT with only nucleons, pions and photons as dynamical degrees of freedom. All contributions from higher mass scales will be encapsulated in the infinite number of higher dimension operators that arise in the momentum and chiral expansions. Some diagrams that will contribute to $np \rightarrow d\gamma$ are shown in Figure 2. Unlike most EFT's that one encounters, higher dimension operators (dim-

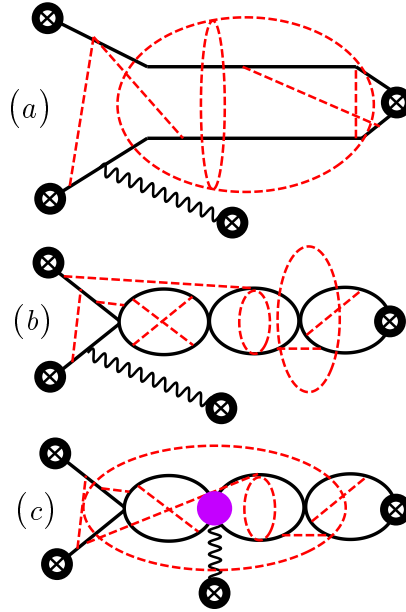


FIGURE 2. Contributions to $np \rightarrow d\gamma$ in a theory with nucleons, pions and photons. Diagram (a) shows a contribution from π -exchange alone, while diagram (b) shows a contribution from π -exchange and from short-distance interactions. Diagram (c) shows a contribution from a local, gauge invariant operator not constrained by nucleon-nucleon scattering data.

6) involving the nucleon field play a central role [2]- [6]. The fact that the deuteron is barely bound, with a binding energy of $B = 2.2$ MeV, requires a fine-tuning between pion exchange and short-distance physics. Naively, one would expect a binding energy set by f_π , the pion decay constant, much larger than one finds in

nature. Therefore, the class of diagrams shown in Figure 2(b) is not expected to be suppressed compared to those in Figure 2(a). In addition, contributions from diagrams shown in Figure 2(c) must be included. These arise from an insertion of operators that are gauge invariant by themselves, and are not related in any way to operators describing nucleon-nucleon scattering. They arise from short-distance physics and have a scale typically set by Λ_χ .

Continuing our descent in energy, if one is interested in this process at energies much less than the pion mass, m_π , then it should be sufficient to use an EFT with only nucleons and photons as dynamical degrees of freedom. All contributions from mass scales greater than m_π will be encapsulated in the infinite number of higher dimension operators that arise in the momentum expansion (chiral symmetry is explicitly broken, leaving isospin symmetry as the only relic of the flavor symmetries). Some diagrams that will contribute to $np \rightarrow d\gamma$ are shown in Figure 3. It is im-

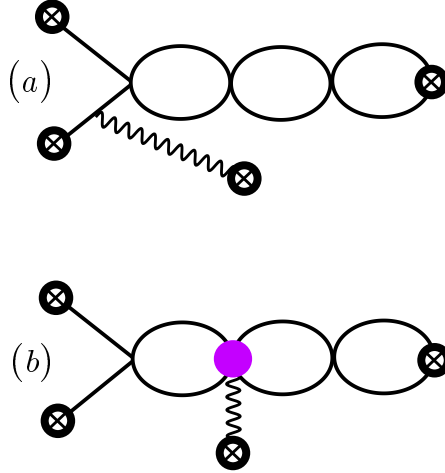


FIGURE 3. Diagrams that contribute to $np \rightarrow d\gamma$ in a theory with nucleons and photons. Diagram (a) shows a contribution from interactions between nucleons. Diagram (b) shows a contribution from a local, gauge invariant operator that does not contribute (at tree-level) to nucleon-nucleon scattering.

portant to realize that nucleon-nucleon scattering described by this EFT uniquely reproduces Effective Range Theory (ERT) [7]. However, for all other observables, such as those involving electroweak gauge fields, ERT (e.g. [7,8]) is seen to be an uncontrolled approximation to EFT (e.g. [9]).

In the following sections I attempt to indicate the status of EFT descriptions in the various energy regimes. Firstly, I will discuss low-energy $|\mathbf{p}| \ll m_\pi$ processes involving two and three nucleons, focusing on the recent high precision calculations that have been performed. Secondly, the issues, results and the present roadblocks to successfully describing the intermediate energy regime $|\mathbf{p}| \gtrsim m_\pi$ are presented. Finally, efforts to translate the understanding gained in EFT developments to many-nucleon systems are described. Such translation is necessary in

order to achieve the ultimate goal of having a perturbative theory of nuclei that faithfully reproduces QCD.

$NP \rightarrow D\gamma$ AT LOW ENERGIES

During the past year there has been considerable focus placed on the radiative capture process $np \rightarrow d\gamma$. Firstly, it was pointed out [10] that the uncertainty in the cross section for $np \rightarrow d\gamma$ contributed significantly to the uncertainties in the predictions of Big-Bang-Nucleosynthesis (BBN) of light element abundances. This resulted from the lack of data in the energy region important for BBN from either $np \rightarrow d\gamma$ or $\gamma d \rightarrow np$. Further, available potential model calculations of these processes [11] are undocumented and error estimates are absent. Tools have recently been developed that allow for a $\sim 1\%$ calculation of the cross section with EFT [13,14]. This was facilitated in part by realizing that it is advantageous to get not only the location of the deuteron pole correct, but also the normalization of the deuteron s-state component. This had long been implemented in the methods of [15,16], and implicit in the construction of Weinberg [2,17], but was only recently implemented in the dimensionally regulated EFT [12]. Finally, there are experimental efforts to measure the small isoscalar $E2_S$ and $M1_S$ amplitudes contributing to $np \rightarrow d\gamma$ using polarized neutrons on polarized protons [18]. At the second workshop on Effective Field Theory in Nuclear Physics held at the *Institute for Nuclear Physics* at the *University of Washington* in 1999, Mannque Rho challenged the participants to compute the $E2_S$ and $M1_S$ amplitudes with the group whose predictions are verified experimentally winning a bottle of exceptional wine. With such a wonderful prize at stake, many workshop participants redirected their efforts to this project. This is now known as the *Rho-challenge*.

$np \rightarrow d\gamma$ for Big-Bang Nucleosynthesis ³

As existing potential model calculations of $np \rightarrow d\gamma$ are undocumented and error estimates unavailable, a 5% uncertainty was assigned to the cross section as input into BBN codes [19]. It would be somewhat dismal if, after several decades of investigations into nuclear physics, the cross section for this process was uncertain at the 5% level. However, EFT calculations have demonstrated that the actual uncertainty is much less than 5%. EFT is a well defined method of calculation and estimates of the uncertainty in a given calculation can be made by considering the magnitude of higher order terms that have been omitted. The expression for the cross section for $np \rightarrow d\gamma$ valid at the $\sim 3\%$ level (with nonrelativistic kinematics) is

$$\sigma = \frac{4\pi\alpha (\gamma^2 + |\mathbf{P}|^2)^3}{\gamma^3 M_N^4 |\mathbf{P}|} \left[|\tilde{X}_{M1}|^2 + |\tilde{X}_{E1}|^2 \right] . \quad (1)$$

³⁾ I thank Gautam Rupak for allowing me to present his results in this section

The isovector $M1_V$ and $E1_V$ amplitudes are

$$|\tilde{X}_{M1}|^2 = \frac{\kappa_1^2 \gamma^4 \left(\frac{1}{a_1} - \gamma\right)^2}{\left(\frac{1}{a_1^2} + |\mathbf{P}|^2\right) (\gamma^2 + |\mathbf{P}|^2)^2} \left[Z_d - r_0 \frac{\left(\frac{\gamma}{a_1} + |\mathbf{P}|^2\right) |\mathbf{P}|^2}{\left(\frac{1}{a_1^2} + |\mathbf{P}|^2\right) \left(\frac{1}{a_1} - \gamma\right)} - \frac{L_{np}}{\kappa_1} \frac{M_N}{2\pi} \frac{\gamma^2 + |\mathbf{P}|^2}{\frac{1}{a_1} - \gamma} \right]$$

$$|\tilde{X}_{E1}|^2 = \frac{|\mathbf{P}|^2 M_N^2 \gamma^4}{(\gamma^2 + |\mathbf{P}|^2)^4} \left[Z_d + \frac{M_N \gamma}{6\pi} \left(\frac{\gamma^2}{3} + |\mathbf{P}|^2 \right) \overline{C}^{(P)} \right], \quad (2)$$

where κ_1 is the isovector nucleon magnetic moment, $a_1 = -23.714 \pm 0.013$ fm is the scattering length in the 1S_0 channel, $r_0 = 2.73 \pm 0.03$ fm is the effective range in the 1S_0 channel, $\gamma = \sqrt{M_N B}$ is the deuteron binding momentum, $\overline{C}^{(P)}$ is a number derivable from the nucleon-nucleon p-wave amplitudes, $Z_d = 1/(1 - \gamma \rho_d)$ is the residue of the 3S_1 nucleon-nucleon amplitude at the deuteron pole, and ρ_d is the effective range in the 3S_1 channel. There is also a contribution from an operator that is not related by gauge invariance to nucleon-nucleon scattering, L_{np} . This is the coefficient of a local operator involving four-nucleon fields and a magnetic photon. For incident neutrons with speed $|v| = 2200$ m/s the cross section for capture by protons at rest is measured to be $\sigma_{\text{cold}}^{\text{expt}} = 334.2 \pm 0.5$ mb [20]. The value of L_{np} is fixed by requiring that the expressions in eqs. (1) and (2) reproduce $\sigma_{\text{cold}}^{\text{expt}}$. The amplitudes in eq. (2) have been computed to one higher order by Rupak [14], including relativistic effects and the appearance of an E1 counterterm, providing a $\sim 1\%$ calculation of $np \rightarrow d\gamma$. Once L_{np} has been fixed, the photo-dissociation cross section $\gamma d \rightarrow np$ can be determined, and is shown in Figure 4. One finds that

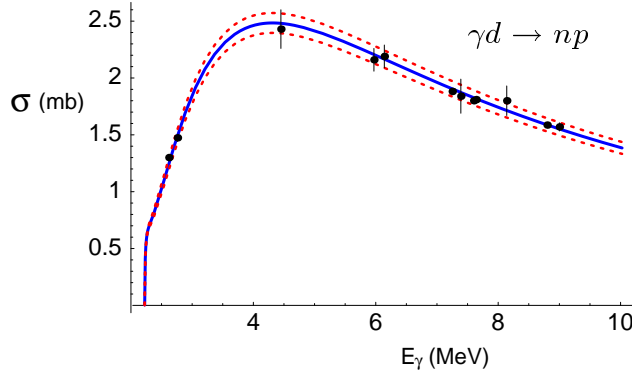


FIGURE 4. The photodissociation cross section for $\gamma d \rightarrow np$. The solid line results from eqs.(1) and (2) [13] with L_{np} determined by the cross section for cold $np \rightarrow d\gamma$. The dashed lines denote the theoretical uncertainty. Rupak has further reduced this uncertainty to below 1% [14].

this relatively simple analytic expression reproduces the data very well, once the counterterm L_{np} has been determined at a given energy. An idea of the convergence of the effective field theory calculation can be obtained from the numerical results of Rupak [14],

$$\sigma(2 \text{ MeV}) = 0.0218 (1 + 0.6389 + 0.0135 - 0.0053 - 0.0001 + \dots) \text{ fm}^2$$

$$\sigma(20 \text{ keV}) = 0.1917 (1 + 0.1076 + 0.0001 + \dots) \text{ fm}^2 \quad , \quad (3)$$

which are both seen to converge rapidly. The cross section at various energies

TABLE 1. $\sigma(np \rightarrow d\gamma)$ as a function of the nucleon center-of-mass energy, E . The asterisk denotes an input.

E (MeV)	total EFT σ (mb) [14]	ENDF σ (mb) [11]
1.264×10^{-8}	334.2 (*)	332.0
5.0×10^{-4}	1.668(0)	1.660
1.0×10^{-3}	1.172(0)	1.193
5.0×10^{-3}	0.4982(0)	0.496
1.0×10^{-2}	0.3324(0)	0.324
5.0×10^{-2}	0.1081(0)	0.108
0.100	0.06352(0)	0.0633
0.500	0.0341(1)	0.0345
1.00	0.0349(4)	0.0342

computed with EFT by Rupak [14], along with those from the on-line nuclear data center [11] are shown in Table 1. As expected the EFT calculation agrees with the numerical values from [11] at the $\sim 1\%$ level.

Isoscalar M1 and E2 Amplitudes in $np \rightarrow d\gamma$

As mentioned earlier, the *Rho Challenge* focused on the $M1_S$ and $E2_S$ isoscalar amplitudes that contribute to $np \rightarrow d\gamma$, so that predictions can be compared with the imminent measurement of polarization observables [18]. Two works were completed soon after the challenge was issued, one by Kubodera, Park, Min, and Rho [21], and one by Chen, Rupak and myself [22].

There are a couple of angular distributions that can be measured in $\vec{n} + \vec{p} \rightarrow d\gamma$, but if in addition, the polarization of the γ can be measured one finds that there is a different cross section for production of right-handed versus left-handed circularly polarized photons. Defining the asymmetry $A^\gamma(\theta)$ to be the ratio of the difference to the sum of these cross sections,

$$A_{\eta_n}^\gamma(\theta) = \eta_n \left[(P_\gamma(M1) + P_\gamma(E2)) \cos \theta + P_\gamma(E1) \sin^2 \theta \right] \quad , \quad (4)$$

where the $P_\gamma(\Pi L)$ are combinations of the $M1_V$, $M1_S$, $E1_V$ and $E2_S$ amplitudes, and η_n is the neutron polarization vector.

The amplitudes and polarizations are computed in two very different ways. In [21] EFT wavefunctions are developed with a coordinate-space cut-off, which are then used to determine matrix elements of the various electric and magnetic multipole operators. Pions appear as dynamical degrees of freedom and determine the long-range part of the nucleon-nucleon interaction. In addition, counterterms are included via short-distance interactions (e.g. “delta-shell” and others) so that the

magnetic and quadrupole moment of the deuteron are recovered. A very different construction is used in [22]. The EFT without pions is used and divergences are dimensionally regulated. As in [21], the four-nucleon-one photon counterterms are chosen to recover the deuteron magnetic and quadrupole moments, to give $P_\gamma(M1) = -7.1 \times 10^{-4}$, $P_\gamma(E2) = -3.5 \times 10^{-4}$ and a total of $P_\gamma = -1.06 \times 10^{-3}$ in the forward direction, approximately 2/3 of the experimentally determined value of [23] $P_\gamma^{\text{expt}} = -(1.5 \pm 0.3) \times 10^{-3}$. Given the large uncertainty in the calculation of the $M1_S$ amplitude, and the uncertainty of the measurement, the two are not inconsistent. $P_\gamma(M1) = -7.1 \times 10^{-4}$ agrees with the results of Burichenko and Kriplovich [24] of $P_\gamma(M1) = -7.0 \times 10^{-4}$ from a Reid soft-core calculation, but is somewhat less than their zero-range calculation of $P_\gamma(M1) = -9.2 \times 10^{-4}$. However, given the large uncertainty in the $M1_S$ amplitude of [22], both values are consistent. $P_\gamma(E2) = -3.5 \times 10^{-4}$ calculated in [22] agrees well with that computed in [21], and therefore these observables do not distinguish between the two EFT methods.

WEAK INTERACTIONS OF THE DEUTERON

Weak interaction processes involving the deuteron are central to current research efforts in nuclear physics. In addition to the accelerator based programs to elucidate the flavor structure of the nucleon, such as the SAMPLE experiments [25] at Bates, the interactions between neutrinos and the deuteron form the core of our efforts to learn about the neutrino and look beyond the standard model of electroweak interactions. Both in production, e.g. $pp \rightarrow de^+\nu_e$, and in detection at SNO (Sudbury Neutrino Observatory), e.g. $\nu_\mu d \rightarrow \nu_\mu np$, charged and neutral current weak interaction matrix elements between the deuteron and continuum states are required.

Much effort over the past few decades has been put into calculating the production mechanism $pp \rightarrow de^+\nu_e$, both from standard non-relativistic quantum mechanics [26], and from sophisticated potential model techniques [27]. Recently, EFT has been applied to this process by Kong and Ravndal [28] and by Park, Kubodera, Min and Rho [29] giving elegant expressions and numerical values of the weak capture cross section that are consistent with previous estimates⁴. The cross section depends somewhat on the value of a four-nucleon-one-weak-gauge-boson interaction, with coefficient $L_{1,A}$, as defined in [31].

The detection reactions, $\nu d \rightarrow np\nu$, $\nu_e d \rightarrow e^- pp$ and $\bar{\nu}_e d \rightarrow e^+ nn$ had been looked at by two groups, Ying, Haxton and Henley (YHH) [32] and Kubodera and Nozawa (KN) [33], using sophisticated potential models. The two sets of calculations differ at the 5% level, due to different treatments of meson-exchange currents (MEC). Recently, Butler and Chen [31] have determined the break-up cross sections with EFT. Only $L_{1,A}$ needs to be fixed in order to perform a $\sim 1\%$ calculation. The YYH and KN numerical results can be recovered with different

⁴) There has also been recent work in [30] that I have so far failed to comprehend.

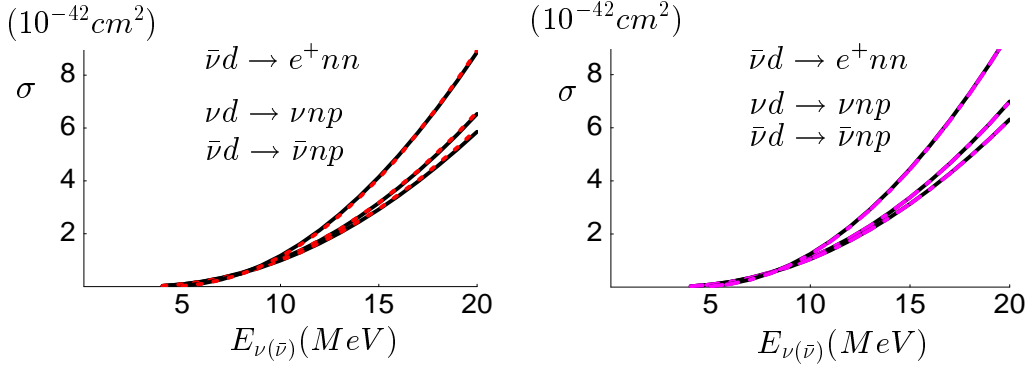


FIGURE 5. Inelastic $\nu(\bar{\nu})d$ cross-sections versus incident $\nu(\bar{\nu})$ energy. The solid curves in the left graph are KN results [33] while the dot-dashed curves, which lie on top of the solid curves, are NLO in EFT with $L_{1,A} = 6.3 \text{ fm}^3$. The solid curves in the right graph are YHH results [32] while the dashed curves, which also lie on top of the solid curves, are NLO in EFT with $L_{1,A} = 1.0 \text{ fm}^3$.

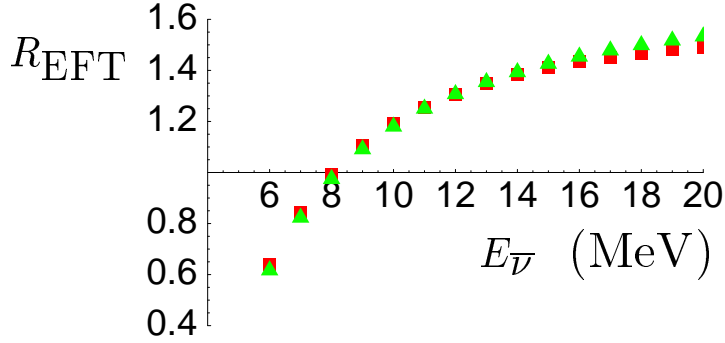


FIGURE 6. The ratio of charged current to neutral current cross sections in $\bar{\nu}d$ scattering versus incident $\bar{\nu}$ energy at NLO in EFT with $L_{1,A} = -20 \text{ fm}^3$ (boxes) and 40 fm^3 (triangles).

choices of $L_{1,A}$, as shown in Figure 5⁵, confirming that the difference between the two potential-model calculations is short-distance in origin. Therefore, to predict the break-up cross section with a precision of better than $\sim 5\%$, one has two options. Firstly, compute the β -decay of tritium, and use this to determine the counterterm $L_{1,A}$ in the EFT, or equivalently the MEC's in the potential models⁶. Secondly, one can perform an experiment to measure one of the break-up cross sections to high accuracy, and thereby extract $L_{1,A}$, or the MEC's. Such an experiment is currently under consideration [34]. An important input into determining if neutrinos are changing flavor as they move out of the sun and to the earth is the ratio of charged current to neutral current cross sections. Figure 6 shows that this ratio, unlike the individual cross sections, is relatively insensitive to the counterterm $L_{1,A}$.

⁵⁾ I thank Malcolm Butler and Jiunn-Wei Chen for allowing me to reproduce their figures

⁶⁾ This method of fixing the MEC's has already been implemented for $pp \rightarrow de^+\nu_e$ [27].

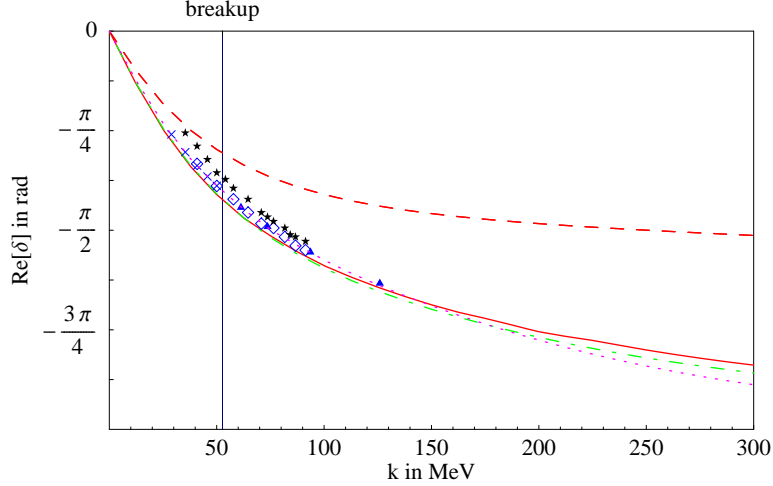


FIGURE 7. $Re(\delta)$ versus incident momentum for Nd scattering in the $J = \frac{3}{2}^+$ channel. The data are taken from the TUNL pd partial wave analysis [44]. The dashed, solid and dotted lines are the LO, NLO and NNLO EFT calculations.

LOW-ENERGY THREE-BODY PROCESSES

Significant progress has been made in understanding three-body systems with EFT [35,36]. A couple of years ago, Bedaque, Hammer and van Kolck⁷ showed very clearly that low-energy Nd scattering in the $J = \frac{3}{2}^+$ channel could be described by EFT using contact interactions alone. One of the more impressive results was the calculation of $a_{\frac{3}{2}}$, the scattering length in the quartet s-wave channel. Bedaque and van Kolck calculated the first three terms to be $a_{\frac{3}{2}} = 5.01 + 1.0 + 0.32 + \dots$ fm where the ellipses denote higher order contributions, that are estimated to be ± 0.1 fm. The calculated $a_{\frac{3}{2}} = 6.32 \pm 0.1$ fm agrees very well⁸ with the experimental $a_{\frac{3}{2}}^{\text{expt}} = 6.35 \pm 0.02$ fm [39]. The first term had been computed in 1957 by Skornyakov and Ter Martirosian [40] while the second term was computed in 1991 by Efimov [41]. The third term had not been computed before and was determined unambiguously from the nucleon-nucleon scattering amplitude [35]. The results of extending this analysis to non-zero energy [35] can be seen in Figure 7 and are found to agree well with data. Scattering in higher partial waves has been examined by Bedaque, Gabbiani and Grißhammer [37] in the theory with only contact interactions between nucleons. A comparison between the EFT calculations⁹, sophisticated potential model calculations and data for one partial wave is shown in Figure 8.

⁷⁾ I thank Paulo Bedaque, Hans-Werner Hammer and Bira van Kolck for allowing me to reproduce their figure.

⁸⁾ Subsequent “second generation” potential-model calculations agree with this result [38].

⁹⁾ I thank Paulo Bedaque, Fabrizio Gabbiani and Harald Grißhammer for allowing me to reproduce their figure.

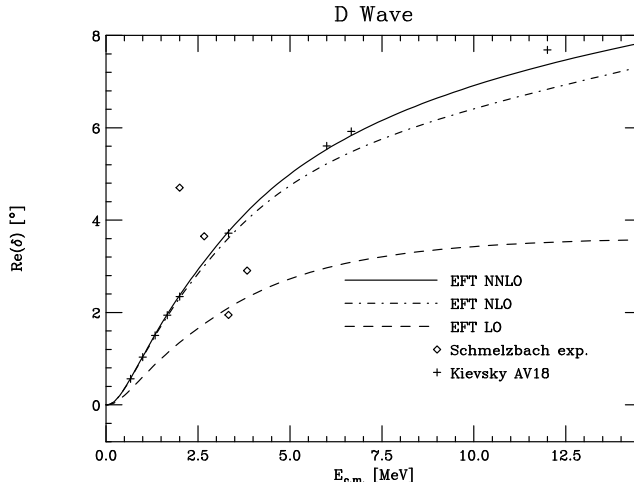


FIGURE 8. $Re(\delta)$ versus incident momentum for Nd scattering in the $L = 2$ quartet channel. The dashed, dot-dashed and solid line is LO, NLO and NNLO. Calculations are shown as crosses [42], while the phase shift analysis is shown by open squares and diamonds [43].

Computations in the spin-doublet channel required much more development as local three-nucleon operators can contribute to the scattering amplitude [36]. The scale-dependence of the counterterm (more commonly known as the three-body force) is quite different from those that are familiar from perturbative field theory. Bedaque, Hammer and van Kolck showed that a single momentum independent counterterm could absorb all cut-off dependence from the leading operators resummed by the integral equation that describe three-body systems. The observed periodicity as a function of scale indicates that if a given calculation is performed with a given value of the cut-off, it is possible that the three-body “force” vanishes, while for a different value of the cut-off the three-body “force” may dominate. Further, the appearance of only one three-body counterterm required to render the scattering amplitude scale independent also naturally explains the *Phillips line* found in potential-models.

As a last comment on the three-body work, the techniques that have been developed in the nuclear physics setting are being applied to atomic systems, most notably scattering lengths and recombination rates in Bose condensates [45].

ISSUES AT HIGHER ENERGIES

The situation regarding the applicability of EFT’s at higher momentum, near or above the pion mass, is much less clear. In Weinberg’s scheme [2], pion exchange and local four-nucleon operators contribute to nucleon-nucleon scattering at the same order in the expansion parameter. A great calculational and conceptual simplification would arise if the exchange of pions between nucleons could be treated in perturbation theory in all partial waves, as suggested by Kaplan, Wise

and myself (KSW) [6]. Unfortunately, one of the more disappointing results found during the past year is that the EFT with perturbative pions [6] appears not to be converging [46] (also, see earlier work by Cohen and Hansen [47]). Fleming, Mehen and Stewart [46] performed an analytic calculation of the NNLO amplitude for nucleon-nucleon scattering in the theory with pions and KSW power-counting [6]. They found large non-analytic contributions that appear to destroy the convergence of the series. In contrast, several computations were performed with Weinberg's power-counting [2] for the nucleon-nucleon potential which appears to give converging amplitudes. However, the formal inconsistency of Weinberg's power-counting remains. Amplitudes are not renormalization (cut-off) independent at any order in Weinberg's expansion, however, the cut-off dependence is found to be numerically small when renormalized at a typical strong interaction scale. Therefore, at this point in time there is no formally consistent, converging, perturbative EFT to describe nuclear interactions for momenta of order or higher than the mass of the pion.

To give you an idea of what has been attempted at these higher energies with both Weinberg and KSW power-counting, let me show you the results obtained for $\gamma d \rightarrow \gamma d$, deuteron Compton scattering. Three-orders in Weinberg's counting have been completed for $\gamma d \rightarrow \gamma d$ at higher energies [48]. The angular distribution of scattering photons at $E_\gamma = 69$ MeV is shown in Figure 9¹⁰. One can see from

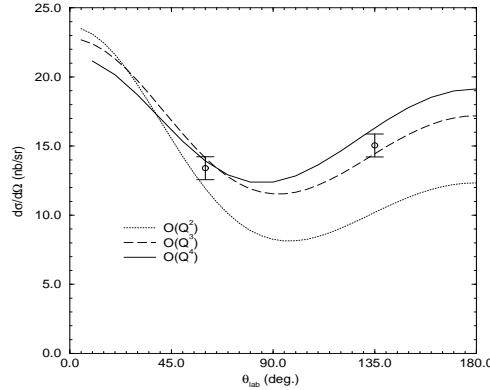


FIGURE 9. $\frac{d\sigma}{d\Omega}$ for $\gamma d \rightarrow \gamma d$ for incident photon energy $E_\gamma = 69$ MeV with Weinberg's power-counting [48]. The dotted, dashed and solid curves are LO, NLO and NNLO. Data is from [49].

Figure 9 that the expansion appears to be converging nicely to the experimental values. Similarly, $\gamma d \rightarrow \gamma d$ has been computed to two orders in KSW power-counting [50], the results of which can be seen in Figure 10. Very good agreement between data and the parameter free-prediction at NLO is found at $E_\gamma = 49$ MeV. The agreement is somewhat worse at $E_\gamma = 69$ MeV, and does not appear to be approaching the data in the same way that the calculation with Weinberg's counting

¹⁰⁾ I thank Daniel Phillips, Silas Beane and Bira van Kolck for allowing me to reproduce their figure.

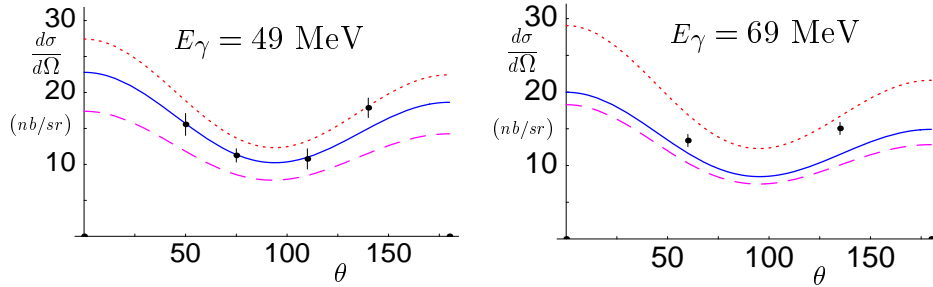


FIGURE 10. $\frac{d\sigma}{d\Omega}$ for γd Compton scattering at incident photon energies of $E_\gamma = 49$ MeV and 69 MeV determined in [50]. The dashed curves are LO. The solid (dotted) curves are NLO with (without) the graphs that contribute to the polarizability of the nucleon. Data is from [49].

appears to. It is clear that higher order calculations must be performed once the perturbative pions versus non-perturbative pions issue is understood, and further, it is clear that more precise data is required at low-energies. It is worth mentioning at this point that neither counting schemes, nor any theoretical calculation that exists at present comes close to reproducing the recent data at $E_\gamma = 95$ MeV [51].

There is much work still to be done in this area.

ON THE ROAD TO NUCLEI

In parallel to the efforts that I have described in the two- and three-body sectors, Haxton and collaborators [52] have been developing techniques to apply the ideas underpinning EFT to the nuclear shell model (efforts are ongoing by others [53] but I will not discuss their work in this talk).

Before I discuss this work I wish to show you the results of a relatively simple but demonstrative calculation by Phillips [54] (see also [55]). To show how the ideas of EFT can be translated into a potential-model mode of thinking, Phillips compared the deuteron quadrupole form factor, presented as T_{20} , computed with the Nijmegen93 potential [56] with that generated by an effective potential, $V_{\text{eff}}^L(r)$ (where L denotes the orbital angular momentum state) and local quadrupole moment counterterm. The effective potential consists of one-pion exchange at long distances and a square-well at short-distances, $V_{\text{eff}}^L(r) = V^{\text{OPE}}(r)$ for $r > R$, and $V_{\text{eff}}^L(r) = V_{0,L}$ for $r < R$. The values of the $V_{0,L}$ are chosen to reproduce the deuteron binding energy, and low-energy nucleon-nucleon scattering for each choice of R . Therefore, the long-distance behavior of the “true” potential and effective potential are identical. Further, the tail of the deuteron wave-function produced by the “true” potential and effective potential are identical. As one is brutalizing the nucleon-nucleon interaction at short-distances while preserving nucleon-nucleon scattering, it is expected that predictions for other observables, such as electromagnetic form factors, will deviate significantly from nature when probing distance scale comparable to or less than R , for reasonable values of R . In addition one expects

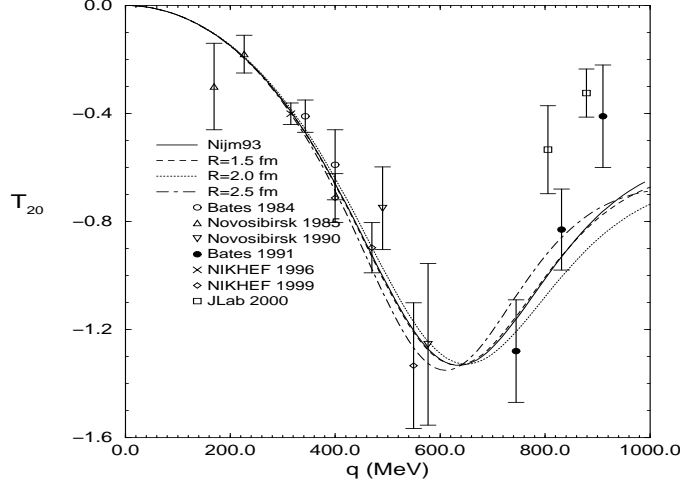


FIGURE 11. T_{20} computed with the Nijmegen93 potential and in the effective theory defined in the text for three values of the spatial cut-off R .

to find that the static moments differ somewhat from nature. It was shown in [9,57] that such short-distance modifications can be compensated by the inclusion of gauge invariant local operators. In the case of the deuteron quadrupole moment it is necessary to introduce a four-nucleon-one-quadrupole-photon operator, that is in no way related to the operators determining nucleon-nucleon scattering. These operators are induced at the chiral symmetry breaking scale, and must be included in any consistent calculation, and in fact, their omission is responsible for the discrepancy between all sophisticated potential model calculations of the deuteron quadrupole moment [58] and its experimental value. Phillips choose a value of this operator to reproduce the observed deuteron quadrupole moment for each value of R , and then predicted T_{20}^{eff} in the effective theory, the results of which are shown in Figure 11¹¹. It is clear from Figure 11 that by fixing parameters in the effective theory to reproduce low-energy observables that, even with a nucleon-nucleon potential that has been brutalized at short-distances, one can essentially recover the “true” form factor over a quite impressive range of momentum transfers. This provides a very clear demonstration that T_{20} is determined largely by the tail of the deuteron wavefunction, the OPE tail of the nucleon-nucleon interaction and the deuteron quadrupole moment. For potential model calculations to accurately determine T_{20} , they must first recover the deuteron quadrupole moment, and to do so they must include a four-nucleon quadrupole operator [9,57].

A very similar exploration is ongoing by Haxton and collaborators [52]. They are attempting to construct a model-space-independent shell model, and are presently focusing on the deuteron to optimize their techniques. The underpinnings of EFT are basis independent, and as such should be able to be implemented in both a plane-wave basis (PWB) or a harmonic oscillator basis (HOB). For a continuum process, obviously the PWB is preferable, but for a bound state it seems reasonable

¹¹⁾ I thank Daniel Phillips for allowing me to reproduce his figure.

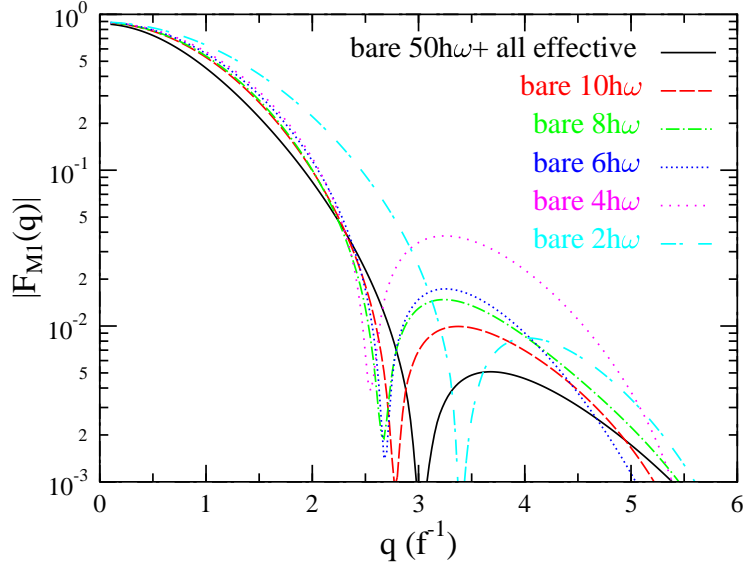


FIGURE 12. The deuteron $M1$ form factor.

that a bound state basis, such as the HOB, will be optimal. In an HOB basis it is natural to integrate out the levels of the HO step by step to allow for an easier calculation in a reduced model-space. As each HO level is removed, the hamiltonian and coefficients of gauge invariant operators are redefined to preserve observables. This is a discrete analog of the renormalization group (RG) implemented in the PWB. In Figure 12¹² the magnetic form factor of the deuteron $F_{M1}(q)$ is shown versus momentum transfer, where the $n = 50$ calculation provides the “true” calculation. The other curves correspond to the same calculation, but with the insertion of the bare $M1$ operator in each reduced model space. The solid line, however, is not just the $n = 50$ calculation but also the calculation from ALL reduced model-spaces when the renormalized $M1$ operator is inserted and NOT the bare operator. Clearly, a discrete RG can be implemented in an HOB.

One of the advantages of constructing a discrete RG for the nuclear shell model would be to greatly reduce the computer time required to compute matrix elements in a nucleus with $A \gg 2$. Presently, efforts are being made to reduce the shell-model space for the deuteron down from $n = 140$, which reproduces the deuteron binding energy perfectly (by construction), down to $n = 20$ or 30 and faithfully reproduce all deuteron observables. Part of the effort is to include the short-range part of the nucleon-nucleon interaction by local operators. If successful, this program will allow for high precision computations of nuclear properties, with greatly increased speed.

¹²⁾ I thank Wick Haxton for allowing me to reproduce his figure.

DISCUSSION

I have tried to give you an overview of a number of important developments of the last year or so. At low-energies, high precision calculations, $\sim 1\%$ have been performed in the two-body sector, and progress is being made toward calculations of similar precision in the three-body sector.

At somewhat higher energies, a formally consistent and converging EFT describing nucleon-nucleon interactions is yet to be uncovered. Weinberg's power-counting is formally ill-defined, yet gives numerical results that appear to be converging. In contrast, KSW power-counting is formally well-defined, yet appears not to be converging! I suspect, as do others, that some sort of union between the two power-countings may in fact be the correct one, but this is merely speculation.

Some of the more interesting developments this year were made in the implementation of EFT ideas in nuclear many-body calculations. There are indications that the EFT techniques may provide a means to compute properties of nuclei presently beyond reach. However, more work is required before any conclusions can be drawn.

REFERENCES

1. G. P. Lepage, Summary talk presented at the INT workshop on *Effective Field Theory in Nuclear Physics II*, edited by P.F. Bedaque, M.J. Savage, R. Seki and U. van Kolck, ISBN-981-02-4181-X.
2. S. Weinberg, *Phys. Lett.* **B251**, 288 (1990); *Nucl. Phys.* **B363**, 3 (1991); *Phys. Lett.* **B295**, 114 (1992).
3. C. Ordonez and U. van Kolck, *Phys. Lett.* **B291**, 459 (1992); C. Ordonez, L. Ray and U. van Kolck, *Phys. Rev. Lett.* **72**, 1982 (1994); *Phys. Rev.* **C53**, 2086 (1996); U. van Kolck, *Phys. Rev.* **C49**, 2932 (1994).
4. T.S. Park, D.P. Min and M. Rho, *Phys. Rev. Lett.* **74**, 4153 (1995); *Nucl. Phys.* **A596**, 515 (1996).
5. D.B. Kaplan, M.J. Savage and M.B. Wise, *Nucl. Phys.* **B478**, 629 (1996).
6. D.B. Kaplan, M.J. Savage and M.B. Wise, *Phys. Lett.* **B424**, 390 (1998); *Nucl. Phys.* **B534**, 329 (1998).
7. H. A. Bethe, *Phys. Rev.* **76**, 38 (1949); H. A. Bethe and C. Longmire, *Phys. Rev.* **77**, 647 (1950).
8. H. P. Noyes, *Nucl. Phys.* **74**, 508 (1965).
9. J.-W. Chen, G. Rupak and M. J. Savage, *Nucl. Phys.* **A653** 386 (1999).
10. S. Burles, K. M. Nollet, J. W. Truran and M. S. Turner, *Phys. Rev. Lett.* **82**, 4176 (1999).
11. ENDF online database at the NNDC Online Data Service, <http://www.nndc.bnl.gov>.
12. D. R. Phillips, G. Rupak, M. J. Savage *Phys. Lett.* **B473**, 209 (2000).
13. J.-W. Chen and M. J. Savage, *Phys. Rev.* **C60**, 065205 (1999).
14. G. Rupak, nucl-th/9911018.

15. T.-S. Park, D.-P. Min and M. Rho, *Phys. Rev. Lett.* **74**, 4153 (1995); *Nucl. Phys.* **A596** 515 (1996).
16. T.-S. Park, K. Kubodera, D.-P. Min, and M. Rho, *Astrophys. Jour.* **507**, 443 (1998); *Phys. Rev.* **C58**, R637 (1998).
17. C. Ordonez and U. van Kolck, *Phys. Lett.* **B291**, 459 (1992); C. Ordonez, L. Ray and U. van Kolck, *Phys. Rev. Lett.* **72**, 1982 (1994); *Phys. Rev.* **C53**, 2086 (1996); U. van Kolck, *Phys. Rev.* **C49**, 2932 (1994).
18. T. M. Muller, *Private Communication*.
19. M. S. Smith, L. H. Kawano and R. A. Malaney, *Astrophys. J. Suppl. Ser.* **85** 219 (1993).
20. A.E. Cox, S.A.R. Wynchank and C.H. Collie, *Nucl. Phys.* **74**, 497 (1965).
21. T.-S. Park, K. Kubodera, D.-P. Min, and M. Rho, *Phys. Lett.* **B472**, 232 (2000).
22. J.-W Chen, G. Rupak and M. J. Savage, *Phys. Lett.* **B464**, 1 (1999).
23. A. N. Bazhenov *et al.*, *Phys. Lett.* **B289**, 17 (1992).
24. A. P. Burichenko and I. B. Khriplovich, *Nucl. Phys.* **A515**, 139 (1990).
25. D. T. Spayde *et al.* (SAMPLE Collaboration) *Phys. Rev. Lett.* **84**, 1106 (2000).
26. J. N. Bahcall and R. M. May, *Ap. J* **55**, 501 (1969).
27. R. Schiavilla *et al.*, *Phys. Rev.* **C58** 1263 (1998).
28. X. Kong and F. Ravndal, *nuc1-th/0004038*; *Nucl. Phys.* **A665** 137 (2000); *Nucl. Phys.* **A656** 421 (1999); *Phys. Lett.* **B470**, 1 (1999).
29. T.-S. Park, K. Kubodera, D.-P. Min and M. Rho, *Nucl. Phys.* **A646**, 83 (1999).
30. A. N. Ivanov, H. Oberhammer, N. I. Troitskaya, and M. Faber *nuc1-th/9910021* and references therein.
31. M. N. Butler and J.-W Chen, *nuc1-th/9905059*.
32. S. Ying, W. C. Haxton and E. M. Henley, *Phys. Rev.* **C45**, 1982 (1992); *Phys. Rev.* **D40**, 3211 (1989).
33. K. Kubodera and S. Nozawa, *Int. J. Mod. Phys.* **E3**, 101 (1994); Y. Kohyama and K. Kubodera, USC(NT)-report-92-1, unpublished.
34. F. Avignone, private communication.
35. P. F. Bedaque and H. W. Griesshammer, *Nucl. Phys.* **A671**, 357 (2000); P.F. Bedaque, H.W. Hammer and U. van Kolck, *Phys. Rev. Lett.* **82**, 463 (1999); *Nucl. Phys.* **A646**, 444 (1999); *Phys. Rev.* **C58**, R641 (1998). P.F. Bedaque and U. van Kolck, *Phys. Lett.* **B428**, 221 (1998).
36. P.F. Bedaque, H.W. Hammer and U. van Kolck, *nuc1-th/9906032*.
37. F. Gabbiani, P. F. Bedaque and H. W. Griesshammer, *nuc1-th/9911034*.
38. J. L. Friar, D. Huber, H. Witala and G. L. Payne, *Acta Phys. Polon.* **B31**, 749 (2000).
39. W. Dilg, L. Koester and W. Nistler, *Phys. Lett.* **B36**, 208 (1971).
40. G. V. Skorniyakov and K. A. Ter-Martirosian, *Sov. Phys. JETP* **4**, 648 (1957).
41. V. Efimov, *Phys. Rev.* **C47**, 1876 (1993).
42. A. Kievsky, S. Rosati, W. Tornow and M. Viviani, *Nucl. Phys.* **A607**, 402 (1996).
43. E. Huttel, W. Arnold, H. Baumgart, H. Berg and G. Clausnitzer, *Nucl. Phys.* **A406**, 443 (1983); P. A. Schmelzbach, W. Grubler, R. E. White, V. Konig, R. Risler and P. Marmier, *Nucl. Phys.* **A197**, 273 (1972).
44. W. Tornow and H. Witala, "Proton-Deuteron Phase-Shift Analysis above the Deuteron Breakup Threshold", Technical Report TUNL XXXVI (1996-97).

45. P. F. Bedaque, E. Braaten and H. W. Hammer, `cond-mat/0002365`. P. F. Bedaque, H. W. Hammer, and U. van Kolck, *Nucl. Phys.* **A646**, 444 (1999).
46. S. Fleming, T. Mehen and I. W. Stewart, `nuc1-th/9911001`; *Phys. Rev.* **C61**, 044005 (2000).
47. T. D. Cohen and J. M. Hansen, `nuc1-th/9908049`; *Phys. Rev.* **C59**, 3047 (1999); *Phys. Rev.* **C59**, 13 (1999); T. D. Cohen, `nuc1-th/9904052`
48. S. R. Beane, M. Malheiro, D. R. Phillips and U. van Kolck, *Nucl. Phys.* **A656**, 367 (1999); private communication.
49. M. A. Lucas, Ph. D. thesis, University of Illinois at Urbana-Champaign (1994)
50. J.-W. Chen, H. W. Griesshammer, M. J. Savage and R. P. Springer, *Nucl. Phys.* **A644**, 245 (1998).
51. D. L. Hornidge *et al.*, *Phys. Rev. Lett.* **84**, 2334 (2000).
52. W. C. Haxton and C. L. Song, `nuc1-th/9907097`; `nuc1-th/9906082`.
53. E. Epelbaum, W. Glockle and U.-G. Meissner, *Nucl. Phys.* **A671**, 295 (2000); *Few Body Syst. Suppl.* **10**, 479 (1999); *Phys. Lett.* **B439**, 1 (1998); E. Epelbaum, W. Glockle, A. Kruger and U.-G. Meissner, *Nucl. Phys.* **A645**, 413 (1999); M. Lutz, `9906028`; H. W. Hammer and R. J. Furnstahl, `nuc1-th/0004043`.
54. D. R. Phillips, `nuc1-th/0004060`.
55. D. R. Phillips and T. D. Cohen, *Nucl. Phys.* **A668**, 45 (2000).
56. V. G. J. Stoks, R. A. M. Klomp, C. P. F. Terheggen and J. J. de Swart, *Phys. Rev.* **C49**, 2950 (1994).
57. D. B. Kaplan, M. J. Savage and M. B. Wise, *Phys. Rev.* **C59**, 617 (1999).
58. R. Machleidt, `nuc1-th/0006014`; R. B. Wiringa, V.G.J. Stoks, R. Schiavilla *Phys. Rev.* **C51**, 38 (1995).